Rapid Communications

Revisited Cassie's law to incorporate microstructural capillary effects

C. M. Mackenzie Dover and K. Sefiane*
School of Engineering, The University of Edinburgh, King's Buildings, Robert Stevenson Road, Edinburgh EH9 3FB, United Kingdom

(Received 20 March 2019; published 7 August 2019)

The equilibrium contact angle and the receding contact angle of water droplets suspended on surfaces comprising arrays of equidistant, uniformly sized square micropillars has been measured with goniometry. Surfaces with distinct pillar size and spacing were fabricated via photolithography and deep reactive-ion etching prior to hydrophobization via the molecular vapor deposition of perflourodecyltrichlorosilane (FDTS). The surfaces exhibited superhydrophobic properties and the measured equilibrium contact angle was compared with the prediction of the Cassie equation based on the measured contact angle on a flat FDTS surface and the surface morphology. A poor agreement between the experimental data and the data predicted by the Cassie equation was found when the spacing between structures was less than the width of the pillars. For more closely spaced structures, the deviation between the measured and predicted values increased. In this roughness region, the measured angle is unchanged by the spacing but the receding angle continues to be dependent on the surface structure. A microscopic examination of the interface between the surface and the droplet revealed that the liquid-gas portion of the contact line was distorted at the pillar edges. The extent of the distortion could not be accurately quantified but it was shown that if the capillary region was assumed to be semicircular and extending half of the width of a pillar in to the liquid-gas region of the contact line, that the contact angle could be predicted well. Moreover, a good prediction of the experimental data of a prior study of droplets on closely spaced circular polydimethylsiloxane micropillar arrays is presented.

DOI: 10.1103/PhysRevFluids.4.081601

I. INTRODUCTION

The wetting of surfaces by liquid droplets is relevant to numerous industrial processes. Microfluidic systems [1], device fabrication [2], inkjet printing [3,4], examination of DNA/RNA [5,6], and heat transfer [7] are all industrial practices where optimization is rooted in the fundamental characterization of wetting. Moreover, the manufacture of ordered experimental surfaces with a known roughness is well within the capabilities of modern micro- and nanofabrication facilities [8]. Therefore, there are a number of studies that examine the effect of such surfaces on the dynamics of liquid droplets with a view to characterize their relationship [9–12].

Generally, the wettability of a surface by a droplet is determined empirically by measuring the angle of the edge of the solid-liquid-vapor region, called the "contact angle." If this angle is greater (less) than 90°, the surface is typically referred to as "hydrophobic" ("hydrophilic"). On a planar surface, the inherent energy of the interface can produce a maximum contact angle of near 120° [13]. The innate wettability of the surface can be enhanced by microstructuring [14] and a droplet wets in two main modes. In the Wenzel mode [15], the liquid from the droplet will fill the space between

*K.Sefiane@ed.ac.uk

the pillars, touching the pillar's substrate. The contact angle θ^* of a droplet in such a configuration can be calculated using the Wenzel equation:

$$\cos\theta^* = r\cos\theta, \tag{1}$$

where θ is the contact angle for a droplet of the same liquid on a chemically equivalent planar surface and r is the roughness ratio; the total surface area of the structured surface as a fraction of the projected area.

In the Cassie-Baxter mode [16], the droplet is suspended atop the pillars and air fills the region between the droplet and the pillar's substrate. For flat-topped pillars the contact angle θ^* can be predicted by Cassie's law:

$$\cos\theta^* = f(\cos\theta + 1) - 1, \tag{2}$$

where θ is the contact angle for a droplet of the same liquid on a chemically equivalent, planar surface and f is the fraction of the liquid/surface interface of the droplet in touch with a flat, solid surface (i.e., tops of pillars):

$$f = \frac{a^2}{(a+b)^2}. \tag{3}$$

For a uniform array of flat, square pillars, a represents the length of the side of a pillar and b is the space between adjacent pillars.

Droplets in the Cassie state can assume an equilibrium contact angle of $>150^\circ$ and such an angle is said to describe superhydrophobicity [13]. There is an ongoing discussion regarding the legitimacy of using equilibrium contact angle as the sole criteria for identifying this phenomenon, however [17–19]. Some studies have argued that the "stickiness" (hysteresis) of a surface should be considered also in characterizing superhydrophobicity [17,18]. Cassie droplets tend to have a low hysteresis [19] compared with Wenzel droplets.

The typical focus of studies that examine Cassie droplets use arrays of widely spaced pillars (low roughness) because these surfaces produce droplets with higher contact angles and with lower hysteresis, and this is of interest particularly for self-cleaning surfaces [20], efficient liquid transfer in microchannels [21] and anti-icing surfaces [22]. Moreover, it is in this roughness region where the Cassie state could switch to the Wenzel state, resulting in a sudden breakdown of superhydrophobicity [23]. It is less common for higher roughness (i.e., where the pillar spacing is less than the width of a pillar) to be considered and in such cases, it is evident that the Cassie equation does not describe the measured contact angle well in the higher (>0.25) roughness region [24–26]. This was illustrated by Erbil and Cansoy [27] where they looked at experimental data from 166 different arrays and found that the majority of data from arrays of circular pillars (up to 77%) and almost half of the data from arrays of square pillars (44%) were not predicted correctly by Cassie's law in its existing form even though the droplets met the criteria to be described as a "Cassie droplet." It has been shown that microscopic changes to the structure of the droplet's contact line can change the macroscale droplet dynamics [28,29]. There is a discussion of the applicability of the Cassie-Baxter equation to various composite surfaces by McHale [30]. McHale presents the example of a droplet on a flat surface comprising nested rings of alternating hydrophobicity and deduces, using an energy minimization approach, that the droplet will adopt the contact angle of the surface on which the contact line of the drop sits, rather than the angle that is predicted by the Cassie-Baxter equation. McHale is in agreement with Gao and McCarthy [31] as well as Extrand [28]; it is interactions at the three-phase contact line that determine the contact angle. Moreover, McHale also discusses pillared surfaces, pointing to the fact that the Cassie-Baxter equation does not incorporate the effect of distortion of the contact line of the liquid suspended between asperities and that the contact angle could be affected by such phenomena. Studies have focused on structuring

the liquid-solid portion of the contact line and consider distortion of the liquid-vapor bridge between pillars only when the pillars are widely spaced [22,32–34].

There is an interest in producing surfaces with high contact angles that are also "sticky" for the fields of driving droplet motion [35,36] and wall-climbing robots [37,38]. Surfaces of this nature are usually complicated to fabricate and require additional manufacturing steps compared with slippery superhydrophobic surfaces [39]. Recent studies have examined the contact line of droplets on a pillared surface with microscopy and have revealed a heavily distorted liquid-vapor region of the contact line between pillars [40,41] and Paxson and Varasani quantified the extent of this region as a function of the surface structure [41]. They showed that for square micropillars a capillary region forms around the edge of the structure that is roughly semicircular over a distance that is approximately half of the length of the side of a pillar. If the square pillars are sufficiently spaced (within one pillar spacing or closer), a capillary "bridge" can form where the capillary regions interact.

In the following we measure the equilibrium contact angle of water droplets on uniform arrays of flat-topped square micropillars of four different areas and with a roughness range of 0.12–0.79. We show that once the pillars are sufficiently close (roughness > 0.20), Cassie's law is a poor predictor of the initial contact angle and additionally, that considering the effect of capillary bridging [capillary bridging effect (CBE)] and by incorporating it into the Cassie equation, we can predict this angle well. The surfaces are superhydrophobic by the definition of initial contact angle, but are demonstrated to have a relatively high contact angle hysteresis and are fabricated in a manner that is identical to slippery superhydrophobic surfaces. Moreover, we show that we can model the results of a separate, prior study of Bhushan *et al.* [25] to further demonstrate the applicability of the modified roughness parameter.

II. PILLARED SURFACES

$1 \times 1\,\mathrm{cm}^2$ square arrays of square pillars of four different areas ($5 \times 5\,\mu\mathrm{m}^2$, $10 \times 10\,\mu\mathrm{m}^2$, $20 \times 20\,\mu\mathrm{m}^2$, and $40 \times 40\,\mu\mathrm{m}^2$) with four different spacings for each pillar area (5, 10, 20, and 40 μm) were fabricated at the Scottish Microelectronics Centre. Pillars were defined using photoresist on a Si wafer (SI-MAT) before Bosch processing was carried out to create pillars $\sim 10\,\mu$m in height with smooth sidewalls. The surfaces were then exposed to perflourodecyltrichlorosilane (FDTS) vapor to form a hydrophobic coating ($\theta = 114.9 \pm 1.8^\circ$). In Fig. 1 a droplet sitting on an array of $20 \times 20\,\mu\mathrm{m}^2$ pillars spaced by 5 μm, a scanning electron microscopy (SEM) image of $10 \times 10\,\mu\mathrm{m}^2$ pillars spaced by 10 μm and a schematic of the experimental setup are shown.

A drop-shape analyzer (DSA 100; Kruss) was used to measure the contact angle of the droplet. Water droplets (25 μl) were deposited on each array before the surface was tilted at 1°/s. The initial contact angle and the angle of the backside of the droplet just prior to the radius of the droplet moving relative to the surface were recorded and this information was used to calculate the hysteresis.

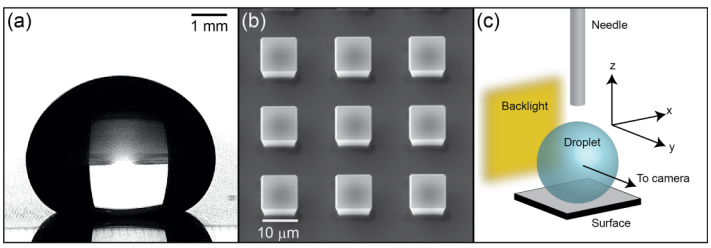

FIG. 1. (a) Side-on goniometer view of droplet on microstructured surface, (b) SEM image of square pillar array, and (c) schematic of goniometer setup.

III. RESULTS

Paxson and Varasani [41] showed that there is a microscopic distortion of the liquid-gas region of the contact line between micropillars ("a capillary bridge") and estimated that the region extends roughly half of a pillar length from the solid-liquid interface. If the spacing is within the length of the side of a square pillar, the capillary bridges will interact. Additionally, optical microscopy imaging of the contact line of our surfaces confirms that for closely spaced pillars, there is a curvature of the air-fluid region between pillars (Fig. 2), although the arc length could not be quantified accurately.

Based on optical microscopy measurements (Fig. 2), the liquid-vapor region is assumed to be semicircular at the edge of the pillar. If the spacing is less than one pillar width, it is assumed that the contact line assumes a pseudocircular shape that has the length of the arc of a semicircle with

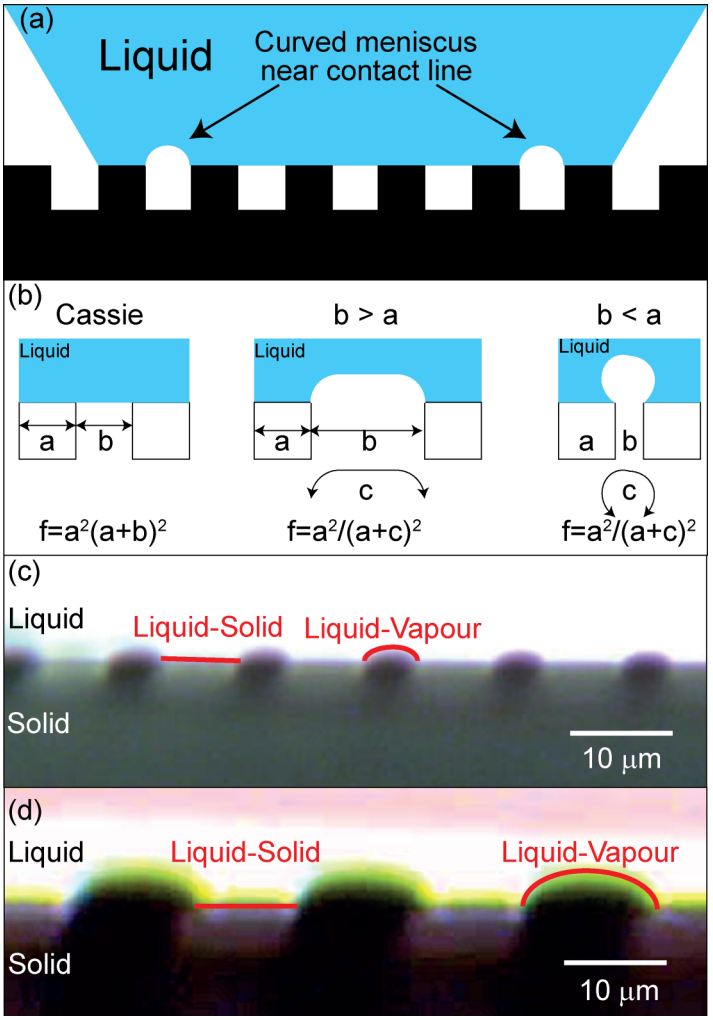

FIG. 2. One-dimensional schematic of (a) contact line of droplet with capillary bridge near droplet contact line. (b) Schematic of assumed contact lines for (left) Cassie model, (middle) spacing greater than pillar width, and (right) interacting capillary bridges. Below: roughness used for each case. Optical microscopy image of contact line of water droplet on $10 \times 10\,\mu m^2$ square pillar arrays with (c) 5 μm and (d) 10 μm spacing showing a curvature of the liquid-vapor interface at the contact line.

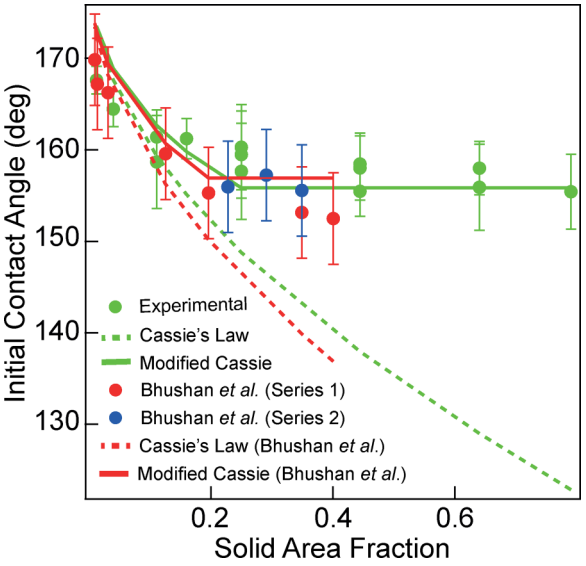

FIG. 3. Equilibrium contact angle as a function of the solid area fraction; experimentally measured from arrays of FDTS coated square pillars (green circles), Cassie's law prediction for experimental FDTS surfaces (broken green line), CBE-modified Cassie's law prefiction for experimental FDTS surfaces (solid green line), data from Bhushan *et al.* [25] (red and blue circles), Cassie's law prediction for Bhushan *et al.* (broken red line), and CBE-modified Cassie's law prediction for Bhushan *et al.* (solid red line).

a diameter of the edge of a pillar. The equilibrium contacted angle is calculated using this new roughness parameter, which can be referred to as the capillary bridge effect (CBE) modified solid area fraction.

The CBE-modified Cassie equation is as follows:

$$\cos\theta^* = g(\cos\theta + 1) - 1, \tag{4}$$

where

$$g = \frac{a^2}{(a+c)^2}, \tag{5}$$

and

$$\begin{aligned} c &= b - a + \tfrac{1}{2}\pi a \quad \text{if } b > a \\ c &= \tfrac{1}{2}\pi a \quad\quad\quad\quad\ \ \text{if } b < a, \end{aligned} \tag{6}$$

where θ^* and θ are as Eq. (2) and a and b are as Eq. (3). In Fig. 2(b) is a schematic describing c as the contact line between pillars that is extended by capillary effects.

Figure 3 shows a plot of the measured initial contact angle as a function of the solid area fraction parameter of the Cassie equation [16] for the four different pillar sizes at various spacings. The range of solid area fraction covered is 0.12–0.79. The experimental data (green circles) is compared with the prediction made numerically using Cassie's law (broken green line). It can be seen that at low roughness [i.e., when pillars are widely spaced (solid area fraction is between 0 and 0.20)], there is a good agreement between Cassie's law and the experimental data. When the spacing is less than the width of a single pillar, Cassie's law is a poor predictor of the contact angle. The discrepancy between the predicted and measured values of the initial contact angle grows as a function of solid area fraction. The solid green line is the contact angle predicted by Cassie's law with CBE-modified solid area fraction (i.e., replacing the pillar spacing with the predicted length of the capillary bridge). The equation agrees well with the experimental data.

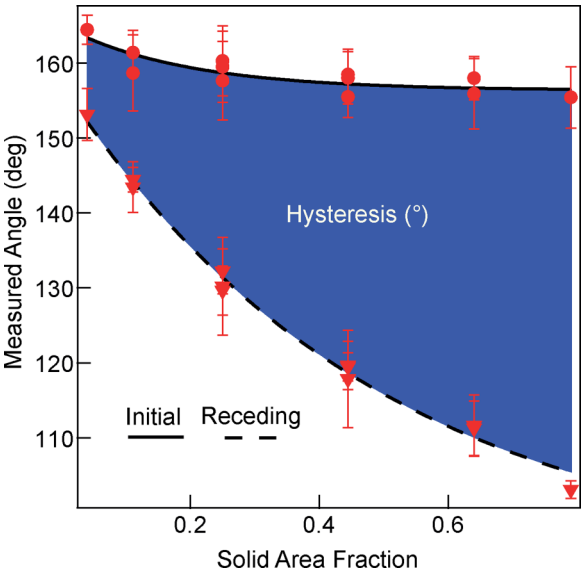

FIG. 4. Initial contact angle (circles, solid black line) and receding angle (triangles, dashed line) plotted against solid area fraction. The blue region illustrates the contact angle hysteresis.

Bushan *et al.* [25] studied uniform arrays of circular polydimethylsiloxane (PDMS) micropillars with diameters of 5 μm (Series 1, red circles, Fig. 3) and 14 μm (Series 2, blue circles, Fig. 3) with a different spacing for each array. The data from this study are plotted as a function of solid area fraction. It is evident that using the CBE-modified solid area fraction is a good fit with the data, whereas the original Cassie-Baxter equation does not fit well for higher solid area fractions (> 0.2).

Figure 4 shows the initial and receding contact angles measured from the experimental substrates described in Fig. 1. It can be seen that for high-solid area fraction arrays (> 0.2) the contact angle remains roughly uniform while the receding angle gets smaller as a function of increasing roughness. This represents a region where the equilibrium wettability is constant (and superhydrophobic) but the hysteresis is not. In the solid area fraction region of 0.2–0.79, the initial contact angle remains $\sim 157^\circ$ while the hysteresis increases from 15° to 55°.

The equilibrium contact angles of droplets on uniform (size and spacing) square arrays of flat-topped square pillars with four different surface areas ($5 \times 5\,\mu m^2$, $10 \times 10\,\mu m^2$, $20 \times 20\,\mu m^2$, and $40 \times 40\,\mu m^2$) and spacings (5, 10, 20, and 40 μm) were investigated. The surfaces represented a roughness range of 0.12–0.79. It was demonstrated that Cassie's law was a poor predictor of the initial contact angle for higher solid area fractions (>0.2). A semicircular capillary bridge was assumed with a radius of the width half of one square pillar. Modifying the solid area fraction in this manner allowed the accurate numerical deduction of the contact angle for our data. Moreover, we are able to predict the experimental initial contact angle from a previous study of arrays of PDMS micropillars more accurately than the conventional Cassie equation. Finally, it is shown that when solid area fraction > 0.2, the initial contact angle will remain stable with increasing solid area fraction but the receding angle will decrease.

IV. CONCLUSIONS

This study shows that superhydrophobic surfaces with a tunable and large hysteresis can be produced with straightforward fabrication steps and that the shape of the liquid-vapor region can strongly influence the droplet dynamics, particularly for tightly packed arrays supporting droplets in the Cassie state. It should be noted that this is not a "one size fits all" solution to a discrepancy

between experimental data and the Cassie equation. The liquid-vapor portion of the contact is likely varied and complicated and future studies should probe the contact line at the microscale and quantify this region as a function of surface structure and the surface energy associated with the chemistry of the interface.

ACKNOWLEDGMENTS

The authors would like to thank MEMSSTAR for providing assistance with sample coatings. This work was funded by EPSRC, Grant No. RA3401.

[1] C. Choi, D. I. Yu, and M. Kim, Surface wettability effect on flow pattern and pressure drop in adiabatic two-phase flows in rectangular microchannels with T-junction mixer, Exp. Therm. Fluid. Sci. **35**, 1086 (2011).
[2] K. Osari, N. Unno, J. Taniguchi, K. Macinaga, T. Ohsaki, and N. Sakai, Evaluation of filling behavior on UV nanoimprint lithography using release coating, Microelectron. Eng. **87**, 918 (2010).
[3] P. Calvert, Inkjet printing for materials and devices, Chem. Mater. **13**, 3299 (2001).
[4] J. Park and J. Moon, Control of colloidal particle deposit patterns within picoliter droplets ejected by ink-jet printing, Langmuir **22**, 3506 (2006).
[5] M. Schena, D. Shalon, R. W. Davis, and P. O. Brown, Quantitative monitoring of gene expression patterns with a complementary DNA microarray, Science **270**, 467 (1995).
[6] V. Dugas, J. Broutin, and E. Souteyrand, Droplet evaporation study applied to DNA chip manufacturing, Langmuir **21**, 9130 (2005).
[7] W. Jai and H. H. Qiu, Experimental investigation of droplet dynamics and heat transfer in spray cooling, Exp. Therm. Fluid. Sci. **27**, 829 (2003).
[8] S. Tawfick, M. De Volder, D. Copic, S. J. Park, C. R. Oliver, E. S. Polsen, M. J. Roberts, and A. J. Hart, Engineering of micro- and nanostructured surfaces with anisotropic geometries and properties, Adv. Mater. **24**, 1628 (2012).
[9] C. Mackenzie-Dover, G. Duursma, K. Sefiane, J. Christy, and J. Terry, Effect of micropillar spacing and temperature of substrate on contact angle dynamics, Heat Transfer Eng. **40**, 794 (2018).
[10] Y. H. Yeong, A. Milonis, E. Loth, and I. S. Bayer, Microscopic receding contact line dynamics on pillar and irregular superhydrophobic surfaces, Sci. Rep. **5**, 8384 (2015).
[11] Y. Q. Zu and Y. Y. Yan, Single droplet on micro square-post patterned surfaces-theoretical model and numerical simulation, Sci. Rep. **6**, 19281 (2016).
[12] C. W. Yao, T. P. Garvin, J. L. Alvarado, A. M. Jacobi, B. G. Jones, and C. P. Marsh, Droplet contact angle behaviour on a hybrid surface with hydrophobic and hydrophillic properties, Appl. Phys. Lett. **101**, 111605 (2012).
[13] N. J. Shirtcliffe, G. Mchale, S. Atherton, and M. I. Newton, An introduction to superhydrophobicity, Adv. Colloid Interface Sci. **161**, 124 (2010).
[14] G. McHale, N. J. Shirtcliffe, and M. I. Newton, Super-hydrophobic and super-wetting surfaces: Analytical potenial? Analyst **129**, 284 (2004).
[15] R. N. Wenzel, Resistance of solid surfaces to wetting by water, Ind. Eng. Chem. **28**, 988 (1936).
[16] A. B. D. Cassie and S. Baxter, Wettability of porous surfaces, Trans. Faraday Soc. **40**, 546 (1944).
[17] K. Y. Law, Definitions for hydrophilicity, hydrophobicity, and superhydrophobicity: Getting the basics right, J. Phys. Chem. Lett. **5**, 686 (2014).
[18] L. Gao and T. J. McCarthy, Teflon is hydrophilic. Comments and definitions of hydrophobic, shear versus tensile hydrophobicity, and wettability characterisation, Langmuir **24**, 9183 (2008).
[19] N. A. Patankar, Hysteresis with regard to Cassie and Wenzel states on superhydrophobic surfaces, Langmuir, **26**, 7498 (2010).

[20] B. Bhurat and Y. C. Jung, Natural and biomimetic artificial surfaces for superhydrophobicity, self-cleaning, low adhesion, and drag reduction, Prog. Mater. Sci. **56**, 1 (2011).
[21] J. Kim and C.-J. Kim, Nanostructured surfaces for dramatic reduction of flow resistance in droplet-based microfluidics, in *Proceedings of the 15th IEEE International Conference on Micro Electro Mechanical Systems, Las Vegas, 2002* (unpublished), p. 479.
[22] L. Afferante and G. Carbone, The effect of drop volume and micropillar shape on the apparent contact angle of ordered microstructured surfaces, Soft Matter **10**, 3906 (2014).
[23] B. Zhang, X. Chen, J. Dobnikar, Z. Wang, and X. Zhang, Spontaneous Wenzel to Cassie dewetting transition on structured surfaces, Phys. Rev. Fluids **1**, 073904 (2016).
[24] Q. Zheng, C. Lv, P. Hao, and J. Sheridan, Small is beautiful, and dry, Sci. China Phys. Mech. **53**, 2245 (2010).
[25] B. Bhushan, M. Nosovsky, and Y. C. Jung, Towards optimization of patterned superhydrophobic surfaces, J. R. Soc. Interface **4**, 643 (2007).
[26] G. Wang, Z. Jai, and H. Yang, Stability of a water droplet on micropillared hydrophobic surfaces, Colloid Polym. Sci. **294**, 851 (2016).
[27] H. Y. Erbil and C. Elif Cansoy, Range of applicability of the Wenzel and Cassie-Baxter equations for superhydrophobic surfaces, Langmuir **25**, 14135 (2009).
[28] C. W. Extrand, Contact angles and hysteresis on surfaces with chemically heterogeneous islands, Langmuir **19**, 3793 (2003).
[29] M. Iwamatsu, Contact angle hysteresis of cylindrical drops on chemically heterogeneous striped surfaces, J. Colloid Interface Sci. **297**, 772 (2006).
[30] G. McHale, Cassie and Wenzel: Were they really so wrong?, Langmuir **23**, 8200 (2007).
[31] L. Gao and T. J. McCarthy, How Wenzel and Cassie were wrong, Langmuir **23**, 3762 (2007).
[32] T. Lui, Y. Li, X. Li, and W. Sun, Mechanism study on transition of Cassie droplets to Wenzel state after meniscus touching substrate of pillars, J. Phys. Chem. C **121**, 9802 (2017).
[33] A. J. B. Milne and A. Amirfazli, The Cassie equation: How it is meant to be used, Adv. Colloid Interface Sci. **170**, 48 (2012).
[34] Q. Zheng and C. Lu, Size effects of surface roughness to superhydrophobicity, Procedia IUTAM **10**, 462 (2014).
[35] X. Song, J. Zhai, Y. Wang, and L. Jaing, Fabrication of superhydrophobic surfaces by self-assembly and their water-adhesion properties, J. Phys. Chem. B **109**, 4048 (2005).
[36] N. A. Malvadkar, M. J. Hancock, K. Sekeroglu, W. J. Dressick, and M. C. Demirel, An engineered anisotropic nanofilm with unidirectional wetting properties, Nat. Mater. **12**, 1023 (2010).
[37] S. Boduroglu, M. Cetinkaya, W. J. Dressick, A. Singh, and M. C. Demirel, Controlling the wettability and adhesion of nanostructured poly-(*p*-xylylene) films, Langmuir **23**, 11391 (2007).
[38] J. Davies, S. Haq, T. Hawke, and J. P. Sargent, A practical approach to the development of a synthetic Gecko tape, Int. J. Adhes. Adhes. **29**, 380 (2009).
[39] X. Wang and R. A. Weiss, A facile method for preparing sticky, hydrophobic polymer surfaces, Langmuir **28**, 3298 (2012).
[40] W. Choi, A. Tuteja, J. M. Mabry, R. E. Cohen, and G. H. McKinley, A modified Cassie-Baxter relationship to explain contact angle hysteresis and anisotropy on non-wetting textured surfaces, J. Colloid Interface Sci. **339**, 208 (2009).
[41] A. Paxson and K. V. Varasani, Self-similarity of contact line depinning from textured surfaces, Nat. Commun. **4**, 1492 (2013).